

Graphenated carbon nanotubes for enhanced electrochemical double layer capacitor performance

Brian R. Stoner, Akshay S. Raut, Billyde Brown, Charles B. Parker, and Jeffrey T. Glass

Citation: [Applied Physics Letters](#) **99**, 183104 (2011); doi: 10.1063/1.3657514

View online: <http://dx.doi.org/10.1063/1.3657514>

View Table of Contents: <http://scitation.aip.org/content/aip/journal/apl/99/18?ver=pdfcov>

Published by the [AIP Publishing](#)

Articles you may be interested in

[Solvothermal synthesis of NiAl double hydroxide microspheres on a nickel foam-graphene as an electrode material for pseudo-capacitors](#)

[AIP Advances](#) **4**, 097122 (2014); 10.1063/1.4896125

[Paper-based ultracapacitors with carbon nanotubes-graphene composites](#)

[J. Appl. Phys.](#) **115**, 164301 (2014); 10.1063/1.4871290

[Effect of nano-filler on the performance of multiwalled carbon nanotubes based electrochemical double layer capacitors](#)

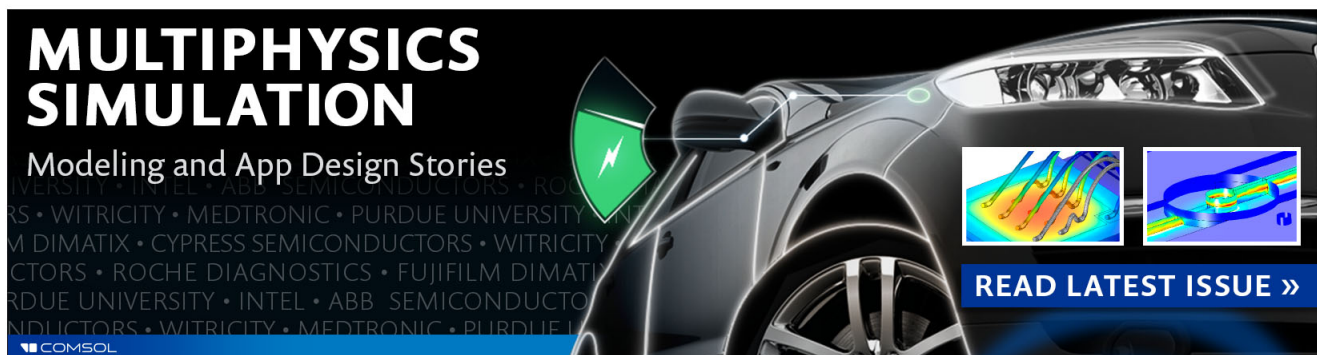
[J. Renewable Sustainable Energy](#) **6**, 013108 (2014); 10.1063/1.4861889

[Composite electrodes of activated carbon derived from cassava peel and carbon nanotubes for supercapacitor applications](#)

[AIP Conf. Proc.](#) **1554**, 70 (2013); 10.1063/1.4820286

[High-performance symmetric electrochemical capacitor based on graphene foam and nanostructured manganese oxide](#)

[AIP Advances](#) **3**, 082118 (2013); 10.1063/1.4819270

The advertisement features a dark background with a car's front end on the right. On the left, the text 'MULTIPHYSICS SIMULATION' is written in large, bold, white letters. Below it, 'Modeling and App Design Stories' is written in a smaller white font. A green shield with a white lightning bolt is positioned to the left of the car. Two small inset images show simulation results: one with a color gradient and another with a blue and yellow pattern. At the bottom right, a blue button with white text says 'READ LATEST ISSUE >>'. The COMSOL logo is in the bottom left corner.

**MULTIPHYSICS
SIMULATION**
Modeling and App Design Stories

READ LATEST ISSUE >>

COMSOL

Graphenated carbon nanotubes for enhanced electrochemical double layer capacitor performance

Brian R. Stoner,^{1,2} Akshay S. Raut,¹ Billyde Brown,¹ Charles B. Parker,^{1,a)} and Jeffrey T. Glass¹

¹Department of Electrical and Computer Engineering, Duke University, Durham, North Carolina 27708, USA

²RTI International, Center for Materials & Electronic Technologies, RTP, North Carolina 27709, USA

(Received 19 August 2011; accepted 7 October 2011; published online 2 November 2011)

This letter reports on nucleation and growth of graphene foliates protruding from the sidewalls of aligned carbon nanotubes (CNTs) and their impact on the electrochemical double-layer capacitance. Arrays of CNTs were grown for different time intervals, resulting in an increasing density of graphene foliates with deposition time. The samples were characterized using electrochemical impedance spectroscopy, scanning electron microscopy, and transmission electron microscopy. Both low and high frequency capacitance increased with increasing foliate density. A microstructural classification is proposed to explain the role of graphene edges, three-dimensional organization, and other features of hybrid carbon systems on their electrochemical properties.

© 2011 American Institute of Physics. [doi:10.1063/1.3657514]

Electrochemical double-layer capacitors or “supercapacitors” are gaining in popularity for applications ranging from hybrid structures in automotive energy storage to load leveling in power transmission.^{1,2} Electrodes for neural stimulation also require high capacitance with both faradaic and non-faradaic components, and thus may benefit from improvements in electrochemical double layer capacitors.³ To optimize such capacitors, high charge density materials on the nano- and/or micro-scale are required, inspiring opportunities to engineer structures that integrate improvements on both scales. Recently, our team reported on the growth and characterization of graphene foliates along the length of vertically aligned carbon nanotubes (CNTs).⁴ The report demonstrated the nucleation and growth of graphene foliates of varying density along carbon CNT sidewalls. Yu *et al.*⁵ also observed high density multi-layer graphene chemically bound to CNTs and examined their electronic and optoelectronic properties. In the present work, structures with varying foliate density are achieved and double layer capacitance is examined to provide insights for electrode applications. A microstructural classification scheme is also proposed to describe the role of graphene edges, three-dimensional (3D) organization, and other features of hybrid carbon systems on their electrochemical properties.

The fundamental advantage of an integrated graphene-CNT structure is the high surface area three-dimensional framework of the CNTs coupled with the high edge density of graphene. Graphene edges provide significantly higher charge density and reactivity than the basal plane, but they are difficult to arrange in a three-dimensional, high volume-density geometry. CNTs are readily aligned in a high density geometry (i.e., a vertically aligned forest)⁶ but lack high charge density surfaces—the sidewalls of the CNTs are similar to the basal plane of graphene and exhibit low charge density except where edge defects exist. For example, Rice and McCreery⁷ and others^{8–11} have reported that the capaci-

tance expected for the basal plane of graphene vs. the edges is 3 vs. 50 to 70 $\mu\text{F}/\text{cm}^2$, respectively. Integrating the properties of these two nanostructures by growing protrusions or foliates of graphene from CNT sidewalls provides a means to optimize the hybrid structure, enabling significantly higher charge storage capacity than either of the two materials can achieve on their own. These structures are referred to as “graphenated CNTs” and the individual multi-layer graphene protrusions are referred to as foliates due to the leaf-like nature, growing from the CNT stem.

The details for the graphenated CNT (g-CNT) growth process are described elsewhere.⁴ In summary, they were grown in a 915 MHz microwave plasma enhanced chemical vapor deposition (MPECVD) system, using 50 Å thick iron catalyst on silicon. Prior to growth, the coated substrates were heated to 1050 °C in 150 sccm of NH_3 , followed by striking and stabilizing the plasma at 21 Torr and 2.1 kW of magnetron input power. Substrates were then pretreated for 180 s in the plasma. Following pretreatment, growth of the CNTs was accomplished by changing the gas flow to 150 sccm CH_4 and 50 sccm NH_3 for 60–480 s. As can be seen in Figures 1(a)–1(c), under these conditions, further deposition time increases the foliate density. The inset in Figure 1(c) is a TEM image of a typical foliate, showing a multi-layer graphene structure, coherent with the CNT sidewalls. For the purpose of this study, only the deposition time was varied so as to limit effects of microstructural changes to the underlying CNT framework caused by expanding the process space.

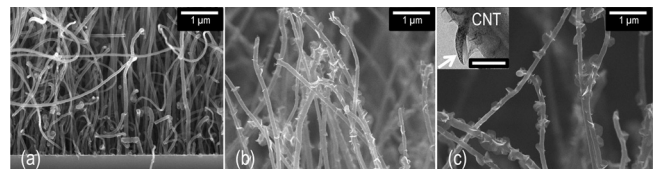


FIG. 1. SEM micrographs of the graphenated CNTs as a function of deposition time. The foliate density increases as a function of deposition time (a) 180 s, (b) 360 s, and (c) 480 s (Inset: TEM of graphene foliate showing hollow CNT core. Foliate indicated by the arrow. Scale bar is 100 nm.)

^{a)}Author to whom correspondence should be addressed. Electronic mail: charles.parker@duke.edu.

The specific capacitance was measured using electrochemical impedance spectroscopy (EIS) between 0.1 Hz and 100 kHz using a 1252 frequency response analyzer and 1287 electrochemical interface (Solartron Analytical) with an Ag-AgCl reference electrode in Model ISF, a biological simulant electrolyte. These CNT-electrodes were initially developed for neural stimulation, thus, a biological simulant¹² was utilized as the electrolyte. Other electrolytes with similar conductivity are expected to provide similar trends in capacitance, and more conductive electrolytes (e.g., 25% KOH a standard aqueous electrolyte used in supercapacitor measurement) should result in a higher initial capacitance due to the lower solution resistance. Future research will evaluate the g-CNT structures in electrolytes optimized for supercapacitor performance. The purpose of this letter is to report on the effect of adding graphene structures to aligned CNTs and the preliminary capacitance trends as a function of foliate density.

Capacitance was obtained by performing EIS scans over the above frequency range and then fitting the impedance magnitude and phase data to the electrode equivalent circuit model shown in Figure 2. A model with a parallel combination of C1 and C2 was examined and provided a better fit to the data than a single R-C model (nonetheless, trends of capacitance vs. graphene foliate density were similar for both cases). Given the hybrid structure of the g-CNT, it can be hypothesized that C1 is associated with the double-layer capacitance (attributed primarily to the exposed graphene edges and edge defects in the CNT sidewalls) and C2 with the pseudo-capacitance (attributed to Faradaic charge-transfer reactions across the interface). However, our goal for the current work is simply to report on the effect of increasing graphene foliate density on capacitance. Future work will examine such an assignment of C1 and C2 to determine its validity. In this circuit model, resistor R2 is the resistance associated with charge transfer and R_s is the equivalent series (or solution) resistance of the electrolyte.

For the purpose of future comparisons, the capacitance data were normalized with respect to area and mass of the exposed g-CNT film. The mass normalized results are shown in Figure 3 and similar trends were observed on a specific nominal area basis (not shown). The data were fit over two frequency regimes: low frequency (1–10 Hz), representing energy storage, or load leveling types of applications for super capacitors; and high frequency (10 Hz–10 kHz), representing applications such as neural stimulation which require

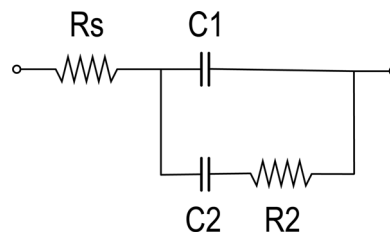


FIG. 2. Equivalent circuit model used for EIS analysis of electrode-electrolyte interface. R_s represents the solution resistance, C_1 the double-layer capacitance due to linear edge defects, C_2 the Faradaic pseudo-capacitance, and R_2 the charge transfer resistance.

pulsed or high frequency operation. The capacitance data for both low and high frequency regimes are plotted in Figure 3(a) as a function of deposition time. Both C1 and C2 show increases as a function of deposition time, which corresponds to foliate density, at low and high frequency, suggesting that optimization of a hybrid CNT-graphene structure should lead to further improvements over either of these two structures optimized on their own.

It is interesting to note that there are measurable increases in capacitance from 60–180 s, before graphene foliates are observable via SEM. The first foliates are not visible until after 180 s, yet there is already a greater than 2× improvement in capacitance. The initial increase in capacitance prior to noticeable formation of graphene foliates may be due to the formation of edge-type defects along the length of the CNTs; defects that form the nucleation sites for the graphene foliates. In fact, there are noticeable undulations along the length of the CNTs prior to foliate formation,⁴ suggesting defects and compressive stress. Fracture following excessive compressive stress is hypothesized as a foliate nucleation mechanism and may provide sufficient edge defects even before foliates are observed via SEM. The primary difference between the high and low frequency data is the charge transfer resistance (R_2), shown in Figure 3(b). In both regimes, R_2 decreases as a function of deposition time and foliate density, representing a decreasing RC time constant for charge transfer, consistent with an increase in the density of reactive graphene edges. However, over the higher frequency regime, R_2 is an order of magnitude lower, suggesting that the R_2 - C_2 combination is more efficient (faster) at higher frequency charge transfer. Ongoing research is designed to isolate this mechanism and study the frequency dependent charge-transfer effect and its correlation to the g-CNT microstructure. In addition, the structures will be

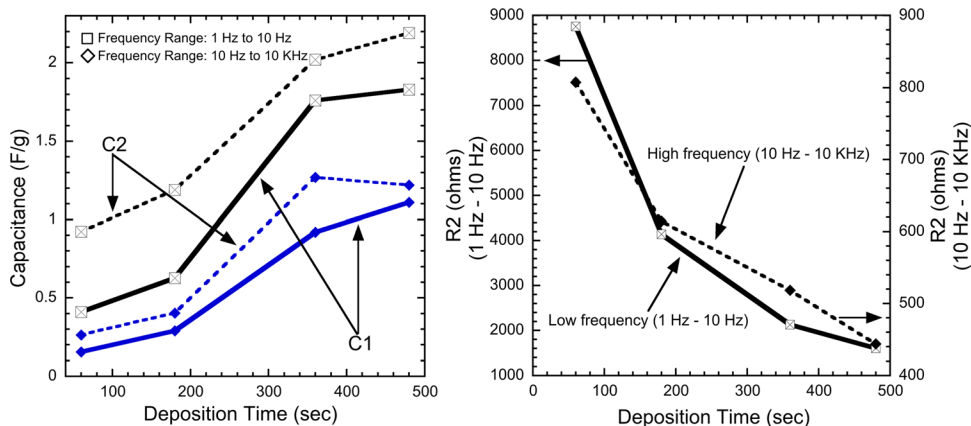


FIG. 3. (Color online) Plots as a function of g-CNT deposition time based on EIS analysis for (a) Capacitance, double-layer (C_1) and pseudo-capacitance (C_2) and (b) charge transfer resistance (R_2).

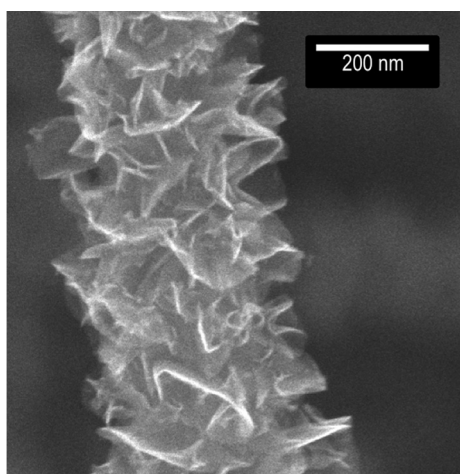


FIG. 4. SEM of an ultra high foliate-density graphenated CNT.

optimized for charge storage. Higher densities of graphene foliates, as shown in Figure 4, will also be examined during that optimization.

To help explain the properties of this CNT-graphene hybrid, Table I outlines a microstructural classification of various carbon nanostructures in the context of their edge or basal plane exposure and whether they are predominantly planar or organized in a 3D network. For a comprehensive review of carbon electrode materials for electrochemical applications, the reader is also referred to the excellent review by McCreery.¹¹ The present research focuses more on the role of specific carbon nanostructures in relationship to the g-CNT hybrid material. The table starts with highly

TABLE I. Microstructural classification of carbon nanostructures for electrochemical capacitors.

Structure schematic	Examples	Description	Reference
	HOPG	Low charge density. Primarily graphene basal plane exposure	Kneten <i>et al.</i> , ¹³ and Inaba <i>et al.</i> ¹⁴
	Graphite	Mostly basal plane exposure with moderate density of edges exposed via steps	Flandrois <i>et al.</i> , ¹⁵ and Zoval <i>et al.</i> ¹⁶
	Herringbone fibers	Mixture of edge and basal plane exposure	Gulijk ¹⁷
	Edge-textured nanosheets	Mostly edge exposure of graphene or graphite nanosheets	Wang <i>et al.</i> ¹⁸
	Activated carbon	Mesoporous structure organized into a 3D network with mixture of edge and basal plane	Ryoo <i>et al.</i> ¹⁹
	g-CNTs	Graphene foliates with both edge and basal plane exposure, organized in 3D structure	Yu <i>et al.</i> ⁵ and Parker <i>et al.</i> ⁴
	Aligned CNTs	3D organization of CNTs with mostly basal plane exposure	Cui <i>et al.</i> ⁶

oriented pyrolytic graphite (HOPG),^{13,14} which is dominated by large areas of basal plane exposure, and then transitions through microstructures that have increasing edge exposure^{15–19} but still are essentially two dimensional (i.e., a single unstacked layer of edges), and then on to three-dimensional organization represented by the g-CNTs (Refs. 4 and 5) and aligned CNTs.⁶ Optimizing this microstructure for double-layer capacitance involves a combination of geometric, microstructural, and electronic factors, all leading to an increase in charge storage capacity. Graphene nanosheets, with their high density of exposed graphene edges, have significantly higher surface charge density than CNTs and HOPG, but are planar structures and difficult to organize in a 3D network. Aligned CNTs provide a well-organized, high surface area 3D geometry, but have primarily basal plane exposure. The g-CNT structure represents a potential maximum in both charge density and surface area, representing the 3D organization of the high charge-density graphene edges, arranged into a larger electrochemically active volume. Thus, on a specific density or nominal area basis, such structures provide the highest capacitance.

In summary, this report presents enhanced electrochemical double-layer capacitance as a function of increasing graphene foliate density along aligned CNTs. Both high and low frequency measurements showed significant increases in capacitance with increasing foliate density. This increase is attributed to the higher surface charge density present at graphene edges in combination with the 3D organization of the graphene foliates achieved via a network of aligned CNTs.

This work was supported in-part by the National Science Foundation through NSF Grant Nos. DMR-1106173 and ECCS 0801942 and also by the RTI Fellows program.

¹A. Kuperman and I. Aharon, *Renewable Sustainable Energy Rev.* **15**(2), 981 (2011).

²J. M. Miller and P. Mitchell, *Ultracapacitor Applications* (The Institution of Engineering and Technology, 2011).

³S. F. Cogan, *Annu. Rev. Biomed. Eng.* **10**(1), 275 (2008).

⁴C. B. Parker, A. S. Raut, B. Brown, B. R. Stoner, and J. T. Glass, "Growth and characterization of graphenated carbon nanotubes," *J. Mater. Res.* (submitted).

⁵K. Yu, G. Lu, Z. Bo, S. Mao, and J. Chen, *J. Phys. Chem. Lett.* **2**(13), 1556 (2011).

⁶H. Cui, O. Zhou, and B. R. Stoner, *J. Appl. Phys.* **88**(10), 6072 (2000).

⁷R. J. Rice and R. L. McCreery, *Anal. Chem.* **61**(15), 1637 (1989).

⁸R. J. Rice, N. M. Pontikos, and R. L. McCreery, *J. Am. Chem. Soc.* **112**(12), 4617 (1990).

⁹J.-P. Randin and E. Yeager, *J. Electrochem. Soc.* **118**(5), 711 (1971).

¹⁰J. R. Miller, R. A. Outlaw, and B. C. Holloway, *Science* **329**(5999), 1637 (2010).

¹¹R. L. McCreery, *Chem. Rev.* **108**(7), 2646 (2008).

¹²S. F. Cogan, P. R. Troyk, J. Ehrlich, C. M. Gasbarro, and T. D. Plante, *J. Neural Eng.* **4**(2), 79 (2007).

¹³K. R. Kneten and R. L. McCreery, *Anal. Chem.* **64**(21), 2518 (1992).

¹⁴M. Inaba, Z. Siroma, A. Funabiki, Z. Ogumi, T. Abe, Y. Mizutani, and M. Asano, *Langmuir* **12**(6), 1535 (1996).

¹⁵S. Flandrois and B. Simon, *Carbon* **37**(2), 165 (1999).

¹⁶J. V. Zoval, J. Lee, S. Gorer, and R. M. Penner, *J. Phys. Chem. B* **102**(7), 1166 (1998).

¹⁷C. van Gulijk, K. M. de Lathouder, and R. Haswell, *Carbon* **44**(14), 2950 (2006).

¹⁸J. Wang, M. Zhu, R. Outlaw, X. Zhao, D. Manos, B. Holloway, and V. Mammana, *Appl. Phys. Lett.* **85**(7), 1265 (2004).

¹⁹R. Ryoo, S. H. Joo, M. Kruk, and M. Jaroniec, *Adv. Mater.* **13**(9), 677 (2001).